JCAMECH

Buckling Behavior of Composite Plates with a Pre-central Circular Delamination Defect under in-Plane Uniaxial Compression

Mohammad Shishesaz[1], Mahsa Kharazi[2], Parvaneh Hosseini[3], Mohammad Hosseini[1,*]

[1] Department of Mechanical Engineering, Shahid Chamran University of Ahvaz, Ahvaz, Iran
[2] Department of Mechanical Engineering, Sahand University of Technology, Sahand New Town Tabriz, P. O. Box: 51335-1996, Iran
[3] Mechanical Engineering Department, Yasouj University, Yasouj, Iran

Abstract

Delamination is one of the most common failure modes in composite structures. In the case of in-plane compressional loading, delamination of a layered flat structure can cause a local buckling in delaminated area which subsequently affects the overall stiffness of the initial structure. This leads to an early failure of the overall structure. Moreover, with an increase in load, the delaminated area may propagate in the post-buckling mode; and consequently, to predict this behavior, a combination of failure modes will be used to predict failure. In this work, the proposed analysis will predict the delamination shape and load carrying capacity of a composite laminated plate during delamination process in post-buckling mode. For this purpose, it is assumed that the composite laminate contains an initial circular delaminated (defected) area. The analysis is performed through a numerical scheme based on finite element method. Results show that in most cases, the onset of crack growth is affected by the first opening mode while it is well probable that during the delamination growth, the effects of other modes dominate the initial primary opening mode. Consequently, during progression of any delamination which may occur as a result of further loading, a jump in failure mode which is predicted in this analysis, may occur. Moreover, the induced results show that the stacking sequence of the delaminated composite plate has a significant effect on the delamination growth and the load carrying capacity of the overall structure.

---

* Corresponding Author.
 Email Address: s.m.hssini@gmail.com

1. Introduction

Growing demand for improving the performance of products such as: less weight, more strength and lower expenses has lead human to the new materials. One of these materials are composites. In recent decades, the use of these materials has grown increasingly. Overall speaking, the structures cannot be manufactured without defects and hence, this puts human life in jeopardy. Consequently, the study of structural defects becomes essential. Failure of composite materials, particularly delamination of composite structures is one of the most important design criteria since it significantly increases the stiffness and load-carrying capacity of the final structure. In structures with in-plane compressive loads, a buckling failure may occurs as a result of excessive load and hence, cause the instability of overall structure. Additionally, buckling of a composite plate with an initial delaminated region can expand the defected region and hence, cause catastrophic results. Obviously, buckling behavior of a laminated composite plate is more complex than that of a perfect-bond plate. Different buckling modes of a laminated plate are generally, local (in delaminated area), global (the whole structure), and/or a combination of both. One of the commonly found failures modes in composites is delamination. In such a plate with an initially delaminated defect area, any compressive load, may cause progression of the delaminated region, where due to complexity of the problem, numerical methods are used to predict their growth. For the cases in which the applied in-plane load is compressional, the presence of the delamination can cause local buckling of the delaminated area. This subsequently affects the overall stiffness of the structure leading to an early failure. Moreover, the delamination may also propagate as the load increases inside the post-buckling region.

In 2001, Nilsson et al. [1] examined delamination buckling and delamination growth in slender composite plates using numerical and laboratory methods. The panels had cross-ply layups with embedded delaminates at various depths, while subjected to compressive (pressure) loading. Their analysis showed that for the delamination at all depths, energy release rate increases during the global buckling. Hwang and Huang [2] in 2005, used a finite element method for nonlinear analysis of laminated composite structures with two delaminations under uniaxial pressure loading. They concluded that if a short delamination occurs at the top of the long delamination (which is located on the middle surface), then the presence the foregoing delamination may significantly reduce the buckling

stress. Three-dimensional finite element model of a delaminated fiber-reinforced composite plate for dynamic analysis was developed by Alnefaie [3] in 2009. His results showed that the internal delamination has a negligible effect on the natural frequencies of delaminated composite plate. Tawk [4] in 2010 developed a hexagonal solid element for the analysis of composite with delamination defects. Finite element method coupled with the virtual crack closure technique, allowed for the calculation of energy release rate for control of crack propagation. The influence of matrix resin on the delaminated composite laminates was studied by Lin [5]. He investigated the onset of delamination. Modified release rate model was employed to capture delamination growth behavior of composite laminates. A new method was proposed by Turon et al. [6] to predict the propagation of delamination in the composite laminates in the framework of Linear Elastic Fracture Mechanics (LEFM). Mixed mode loading was assumed for determination of energy dissipation. Whitcomb [7] analyzed delamination growth of laminated composite plates. He used finite element and energy release rate methods to investigate the post buckling (through the width) behavior of the laminate. Gong et al. [8] developed a nonlinear finite element method to study the buckling and delamination growth behavior of composite laminates which are subjected to four-point bending. Their model was able to predict the load-displacement curve. Delamination growth and buckling behavior of composite laminates which contained an embedded delamination under compressional loading was studied by Wang et al. [9]. They used finite element method to perform their study. Tudeshky et al. [10] employed layerwise plate theory and interface elements to analyze delamination buckling growth under in-plane compressive loading. Their results showed that the proposed numerical method is capable of predicting the delamination growth inside the laminated pates. Many other authors investigated the onset of delamination and its growth in laminated plates under compressive and mixed loading [11-23]. Also, there are many studies in the field of stress analysis of plates and nanoplates [24-32].

Presence or emergence of cracks and discontinuities in the structures and components may be due to several reasons. Naturally, many material production methods result in gaps or discontinuities. Cracks can begin to grow from the gaps and discontinuities and then cause partial rupture and finally lead to failure of the structure. Fracture mechanics is a necessary framework in the field of applied mechanics which may be used to describe the behavior of defected structures under mechanical

loading. Here, one of the most popular and simplest methods to calculate the strain energy release rate (G) is the virtual crack closure technique (VCCT). In this study, due to presence of large displacement, nonlinear analysis is used to predict the delamination growth process. Growth of the delaminated composite plates and their load carrying capacities for symmetrically and non-symmetrically located circular delaminations have been studied as well.

2. Numerical methods for calculating the strain energy release rate

In this study a numerical method based on finite element analysis has been employed to investigate the delamination growth of laminate plates under uniaxial in-plane compressional loading. Based on large deflection which occurs through the post-buckling of the delaminated area and the whole plate, the nonlinear analysis has been performed. Furthermore for modeling the delamination growth, the virtual crack closure technique has been employed. It should be noted that the shape of the delamination changes during the growth while making the delamination front shape to vary continuously during any load increment. Beside of this, the buckling mode of the delaminated area changes simultaneously with delamination growth. This makes the analysis more complicated. The opening criterion of the nodes in the finite element analysis is based on Eq. (1).

$$G_I = \left[\frac{1}{2B \times \Delta a}\right]\left[F_{z1}\Delta w_1 + F_{z2}\Delta w_2\right] \qquad \text{(1)-a}$$

$$G_{II} = \left[\frac{1}{2B \times \Delta a}\right]\left[F_{x1}\Delta u_1 + F_{x2}\Delta u_2\right] \qquad \text{(1)-b}$$

$$G_{III} = \left[\frac{1}{2B \times \Delta a}\right]\left[F_{y1}\Delta v_1 + F_{y2}\Delta v_2\right] \qquad \text{(1)-c}$$

Where F_{z1} and F_{z2} are the components of force at upper and lower nodes in the delaminated area in the z direction. u_1, u_2, v_1, v_2, w_1 and w_2 are the displacement components of the upper and lower layers in the x, y and z direction. Also B and Δa are shown in Fig. 1.

The virtual crack closure technique is one of the most appropriate methods for calculating the strain energy release rate (G) in three-dimensional cracks profiles. Fig. 1 shows a portion of this element surrounded by cubic elements with eight corner nodes. According to this figure, displacement in z, x and y directions are associated with the opening modes I, II and III respectively.
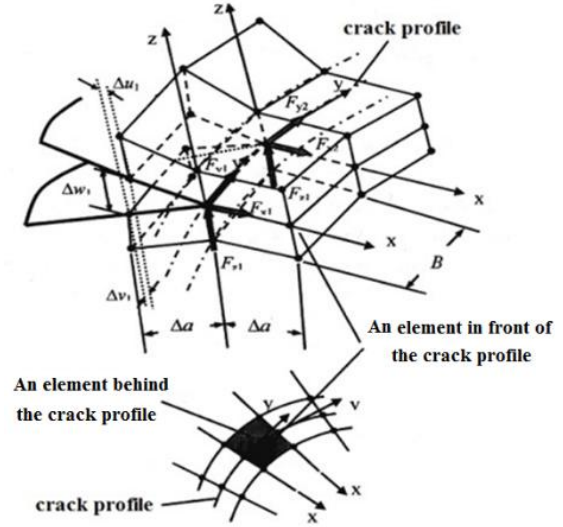

Fig. 1. Elements surrounding a three-dimensional crack tip.

Although a composite material may not fail under a certain mode alone, but presence of other modes, may cause a failure due to interaction of all modes. Therefore in most cases a combination criterion used to evaluate the delamination growth [33] is used. One of these criteria is based on the Reuters's relation which may be written as:

$$MG = \left[\frac{G_I}{G_{IC}}\right]^m + \left[\frac{G_{II}}{G_{IIC}}\right]^n + \left[\frac{G_{III}}{G_{IIIC}}\right]^p \geq 1 \qquad (2)$$

Where G_I, G_{II} and G_{III} are strain energy release rate of the first, second and third mode for a perfectly bonded laminated plate (no delamination). Additionally, G_{IC}, G_{IIC} and G_{IIIC} represent their corresponding critical values, while MG represents the delamination growth criteria. It should be noted that m, n and p are determined experimentally. In this study it is assumed $m = n = p = 1$.

3. Physical and Finite element models

A schematic diagram of the composite plate and location of the embedded circular delamination region is shown in Fig. 2. This figure shows a rectangular composite laminate with a centrally located circular delamination. The radius of the delamination area is 120mm while the length of the square plate is 1000mm. The boundary conditions on all edges of the plate are assumed to be clamped. In all cases (different layup arrangements), the loading is a uniaxial in-plane compression and is applied in terms of displacements on the right and left edges.
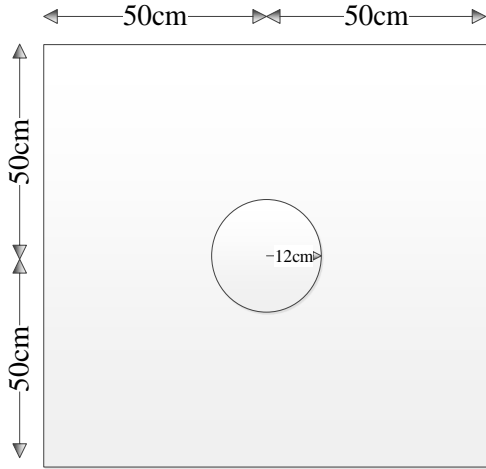
Fig. 2. Initial radius and position of the central delamination in the square laminated plate

To generate the finite element model, ANSYS software V11 was used to model the problem. For this purpose, the 8-node structural solid elements which is designed to model layered thick shells or solids is SOLID46. This element allows for up to 250 different material layers. If more than 250 layers are required, a user-input constitutive matrix option is available. The element may also be stacked as an alternative approach. The element has three degrees of freedom at each node: translations in the nodal *x*, *y* and *z* directions [34]. Contact elements is used to prevent sinking of the upper and lower delamination zones. The material properties and critical values of the strain energy release rate are presented in Table 1 and Table 2, respectively.

Table 1. Mechanical properties of the composite material of carbon – epoxy [33].

E_{11}	109.34 GPa
$E_{33}=E_{22}$	8.82 GPa
$G_{13}=G_{12}$	4.32 GPa
G_{23}	3.20 GPa
$\nu_{13}=\nu_{12}$	0.342
ν_{23}	0.520

Table 2. Critical values of strain energy release rate for carbon – epoxy [33].

G_{IC}	0.306 (N/mm)
G_{IIC}	0.632 (N/mm)
G_{IIIC}	0.817 (N/mm)

Fig. 3 shows the meshed pattern and direction of the applied load in the model. The applied load is imposed in terms of displacement acting on the right and left edges of the composite plate. All boundary conditions are clamped.
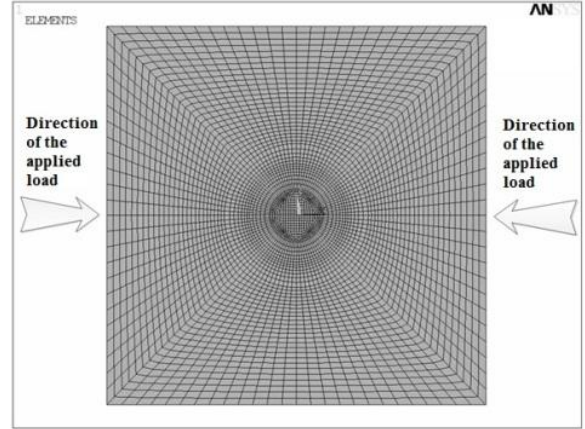

Fig. 3. Meshed pattern and direction of the applied load.

4. Numerical Results

In this section, the strain energy release rate along with its criteria (*MG*) was calculated based on different stacking sequences. The magnitude of the applied load was imposed in terms of right and left edge displacementS. Also delamination growth process and out-of-plane displacement of the delaminated area are shown for each laminated plate.

4.1. The effect of stacking sequence [0//90/90/0/0/90/90/0]

It is assumed that the first sample has a [0//90/90/0/0/90/90/0] stacking sequence where the symbol // denotes the location of delamination. Values of the strain energy release rates for the first stage of crack growth, as well as delamination boundary in the XY plane are shown in Fig. 4. The ordinates show the magnitude of *MG* based on opening criterion of the nodes on the delamination boundary (shown in red) which is given by Eq. (2). The unit of strain energy release rate in this figure (and thereafter) is N/cm. According to this figure, nodes located at $\theta = 0°$ and $\theta = 180°$ (In fact these nodes there are along loading) are opened sooner than other nodes and delamination growth will start from these two locations. Critical displacement for the plate buckling in the first stage is $0.1815mm(\frac{U_x}{U_{xc}} = 0.1444)$ and nodes are opening at $0.563mm(\frac{U_x}{U_{xc}} = 0.4479)$. Additionally, this figure indicates that for a stacking sequence of [0//90/90/0/0/90/90/0] G_I and G_{III} have higher values than G_{II} provided delamination boundary is circular (in the first step of the growth). Therefore failure modes I and III are dominant compared to the second failure mode.

Delamination growth process for this sample is

shown in Fig. 5. As mentioned before, the nodes which are located along the loading direction are opening in the earliest growth step. According to this figure, with the growth process, the nodes located in a direction perpendicular to the direction of the

applied load are opened more, making the growth rate in this direction to dominates the previous one (namely, direction of the applied load). The numbers written on each contour in Fig. 5 represents the nodes opening step.
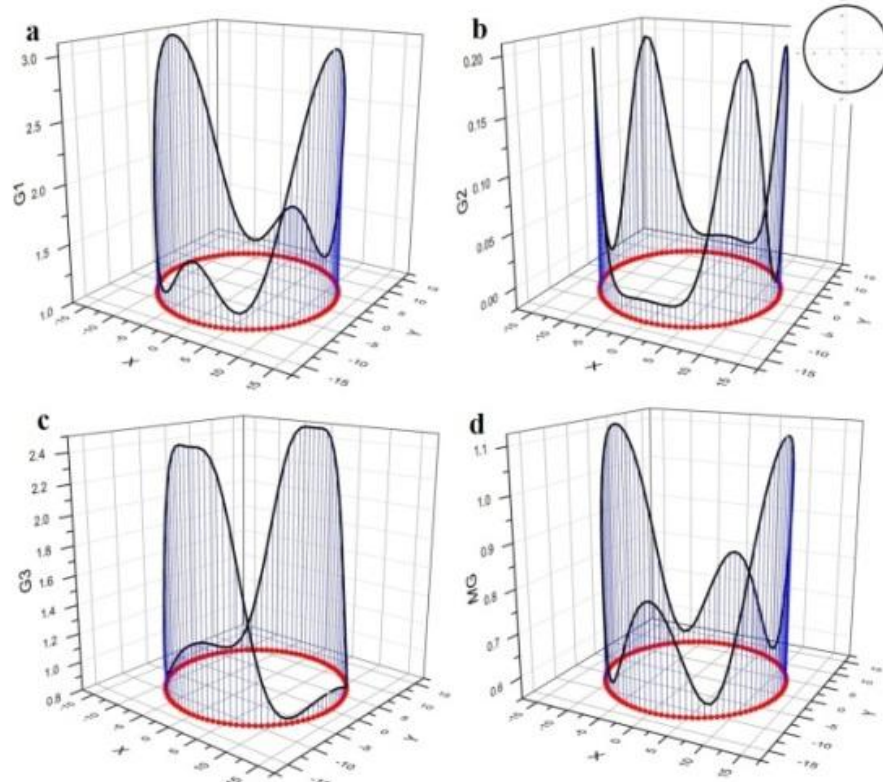

Fig. 4. Strain energy release rate curve of [0//90/90/0/0/90/90/0] sample: a- Strain energy release rate of the first mode, b- Strain energy release rate of the second mode, c- Strain energy release rate of the third mode, d- growth criteria.
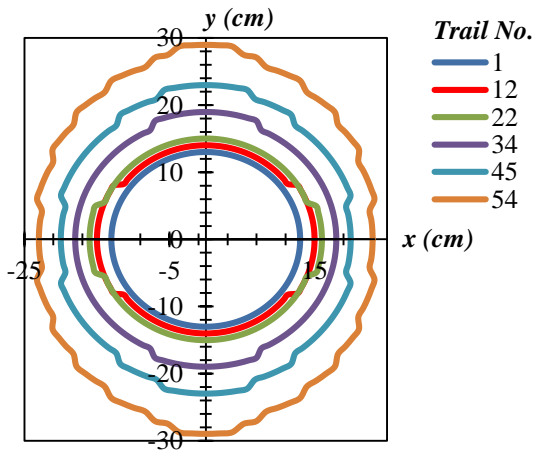
Fig. 5. The delamination growth process in [0//90/90/0/0/90/90/0] sample.

The variation in load carrying capacity versus displacement of the edges is shown in Fig. 6. In this case, plate buckling is local, and hence, the resulting variation is linear. According to this figure, it can be observed that the expansion of the delaminated region due to buckling is unstable, since delamination grows without increasing the compressive load.

In Fig. 6, U_{xc} and N_{xc} represent the critical displacement of the plate edge and critical load carrying of the plate without delamination (perfect-bond plate), respectively. Critical edge displacement and critical load carrying of plate are determined from the first buckling load of the perfect-bond model. U_{xc} and N_{xc} correspond to similar parameters associated with delaminated model under different loading.
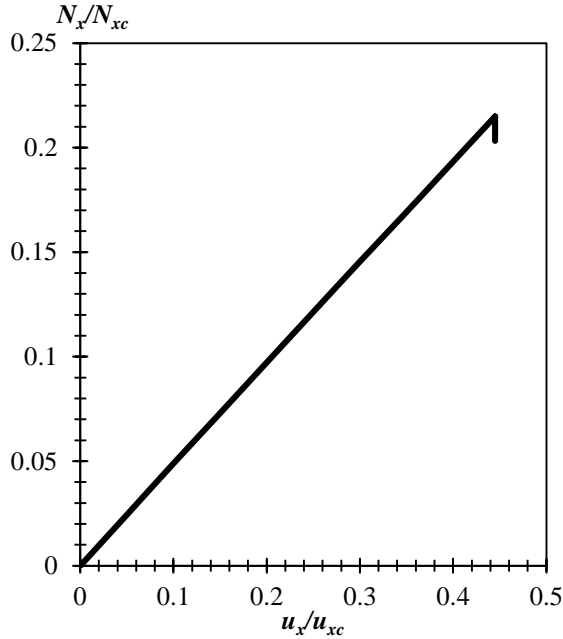
Fig. 6. Variations in the applied load versus displacement of the edges in [0//90/90/0/0/90/90/0] sample.

Out-of-plane displacement of the node located at the center of the plate is presented in Fig. 7. In this figure W is the transverse displacement and H is out of plane displacement of the node located at the center of perfect-bond plate. Wu and Wl are the transverse displacements of the upper and lower layers in the delaminated zone, respectively.

According to Fig. 7, out-of-plane displacement of the node located at the center of the delaminated region increases for $U_x/U_{xc} > 0.1$. Also for $U_x/U_{xc} = 0.45$ the out-of-plane displacement of the top and bottom layers increase while the applied loads at boundary do not vary. In other word, crack growth become unstable.

4.2. Results for stacking sequence of [0/90/90//0/0/90/90/0]

The second sample has [0/90/90//0/0/90/90/0] stacking sequence. The strain energy release rate diagram at the first step of the delamination growth for this stacking sequence is shown in Fig. 8. In this case, nodes located along the loading direction satisfy growth criteria sooner than the others. Results

indicate that local buckling load for the delaminated region at the first step is $1.2366mm$ ($\frac{U_x}{U_{xc}} = 0.9838$) while nodes opening occur at $1.38mm$ ($\frac{U_x}{U_{xc}} = 1.098$).

According to this figure, values of G_I are much greater than those of G_{II} and G_{III}. Therefore, the first failure mode is dominant at the first stage of the growth and the other two modes have very small contribution in delamination growth.

Increasing the displacement load from $1.5mm$ to $1.545mm(\frac{U_x}{U_{xc}} = 1.2291)$, will change the buckling mode from global to local, as shown in Fig. 9. Based on a load step of $1.5mm$, the delaminated layers will buckle, results of which may be a sudden drop in load carrying capacity of the composite plate.

Delamination growth process in the [0/90/90//0/0/90/90/0] sample is shown in Fig. 10. According to this figure, it is observed that the rate of delamination growth is larger in the loading direction.
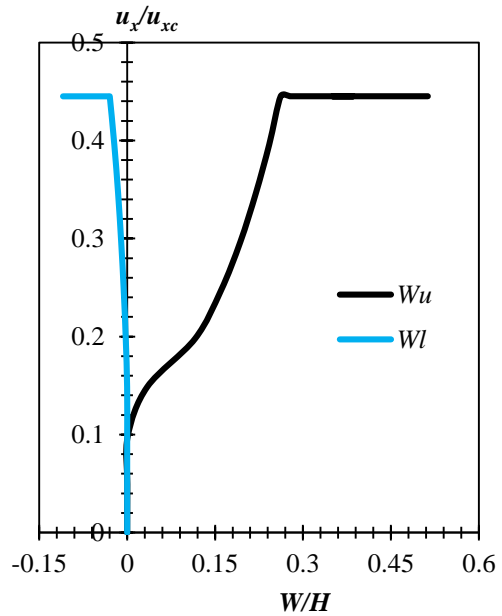

Fig. 7. Out-of-plane displacement of the nodes located at the center of the plate for [0//90/90/0/0/90/90/0] sample.
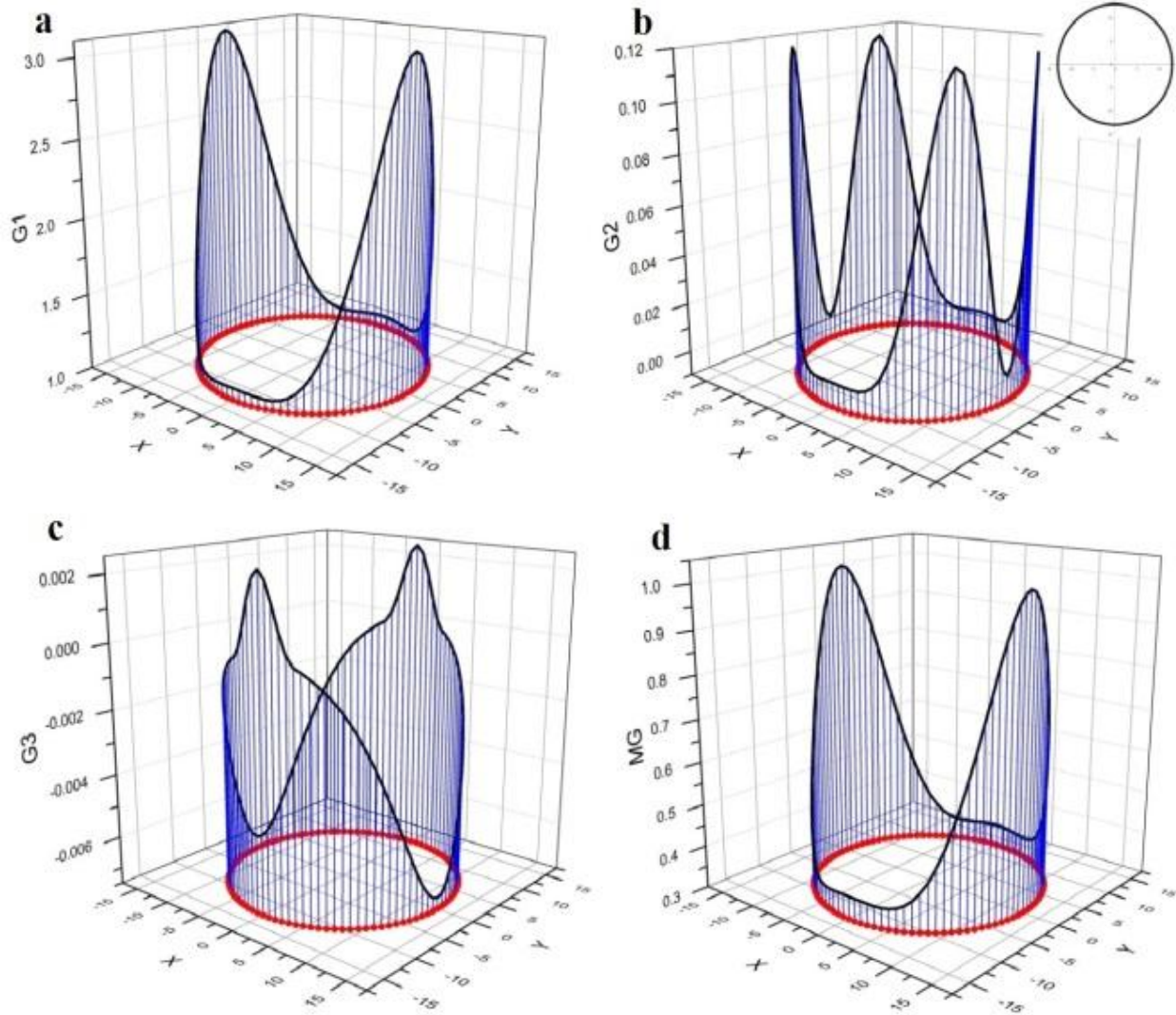
Fig. 8. Strain energy release rate curves for [0/90/90//0/0/90/90/0] sample: a- Strain energy release rate of the first mode, b- Strain energy release rate of the second mode, c- Strain energy release rate of the third mode, d- growth criteria.
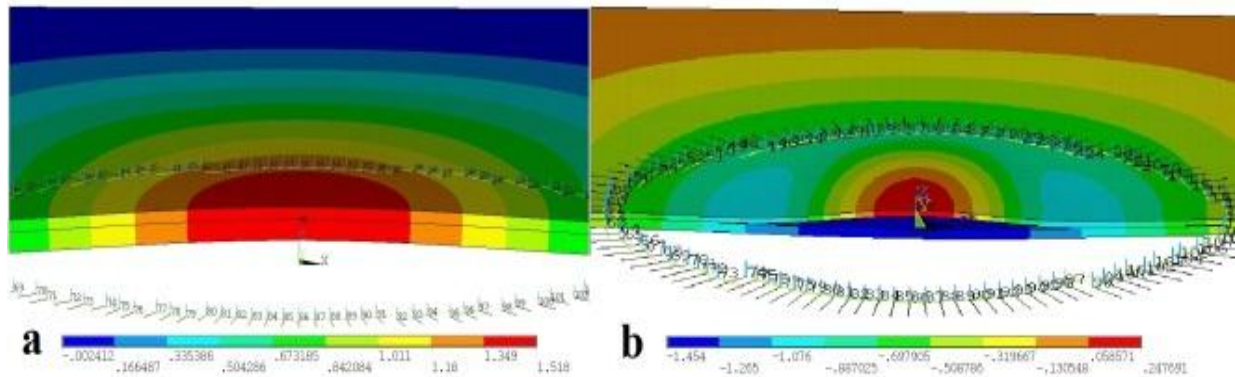

Fig. 9. Change in buckling mode of the [0/90/90//0/0/90/90/0] sample: a- buckling mode under 1.5 mm, b- buckling mode under 1.545 *mm*.
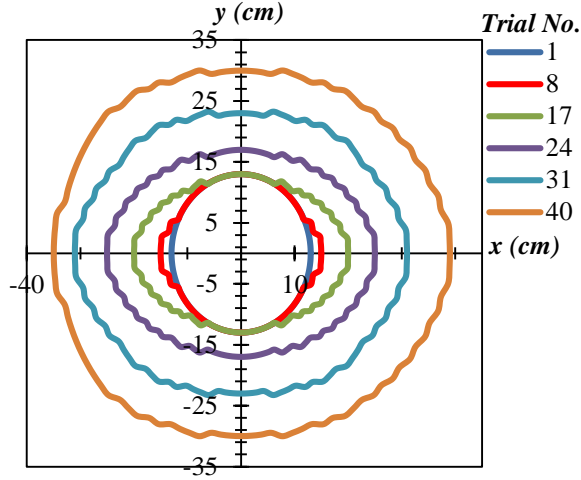
117

Fig. 10. The delamination growth process in [0/90/90//0/0/90/90/0] sample.

As shown in Fig. 11, delamination boundary is not symmetric in the fortieth trial for checking the crack growth due to a change in buckling mode at this step. As observed, the resulting buckling mode beyond this step is a combination of global and local bucklings.
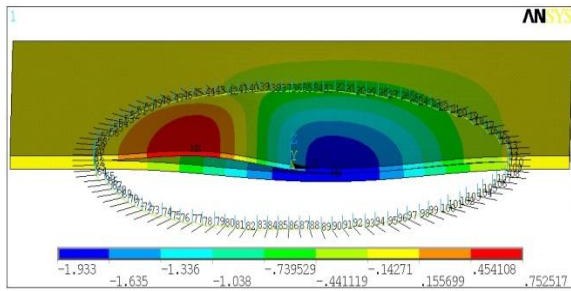

Fig. 11. Buckling mode at the latest stage of delamination growth (fortieth step) in [0/90/90//0/0/90/90/0] sample.

It should be noted that contact elements are used to prevent plate dents in this research. Variation in forces versus the displacement of the edge are shown in Fig. 12. Due to unstable growth of the delamination zone and a change of buckling mode of the whole structure, load carrying capacity experiences a sharp drop in the final step of the analysis for this stacking sequence.

Out-of-plane displacement of the node located at the center of the plate is shown in Fig. 13. This figure confirms the results obtained for the change in buckling mode shown in Fig. 11.
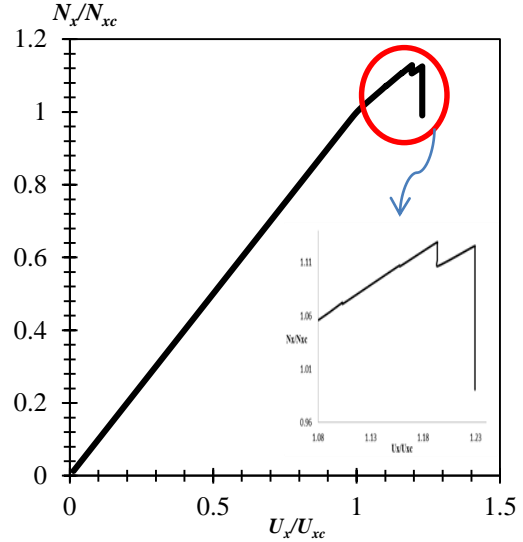

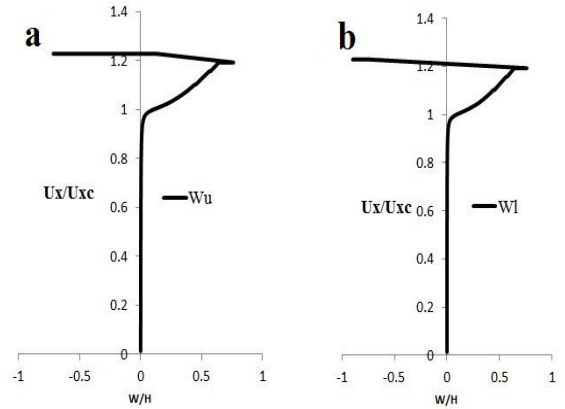Fig. 12. Variation in force based on the edge displacement in [0/90/90//0/0/90/90/0] sample.

Fig. 13. Out-of-plane displacement of the node located at the center of the plate for [0/90/90//0/0/90/90/0] sample: a- Displacement of the node located at the top of the delaminated region, b- Displacement of the node located at the bottom of the delaminated region.

4.3. Results for stacking sequence of [90//0/0/90/90/0/0/90]

According to the numerical results, the buckling load for this laminated plate at the first step is $0.93901mm(\frac{U_x}{U_{xc}} = 0.7750)$ while the nodes are opening at $1.9494mm(\frac{U_x}{U_{xc}} = 1.6090)$. According to Fig. 14, for this stacking sequence, the buckling mode is such that the distribution of G_I and G_{III} are not symmetric with respect to the *y*-axis. Strain energy release rates as well as a plot of delamination growth criteria for this sample are shown in Fig. 14. As observed, all nodes are opened in the first step while the first opening mode is dominant compared to the other two (second

and third) modes. The buckling mode of the plate is   shown in Fig. 15.
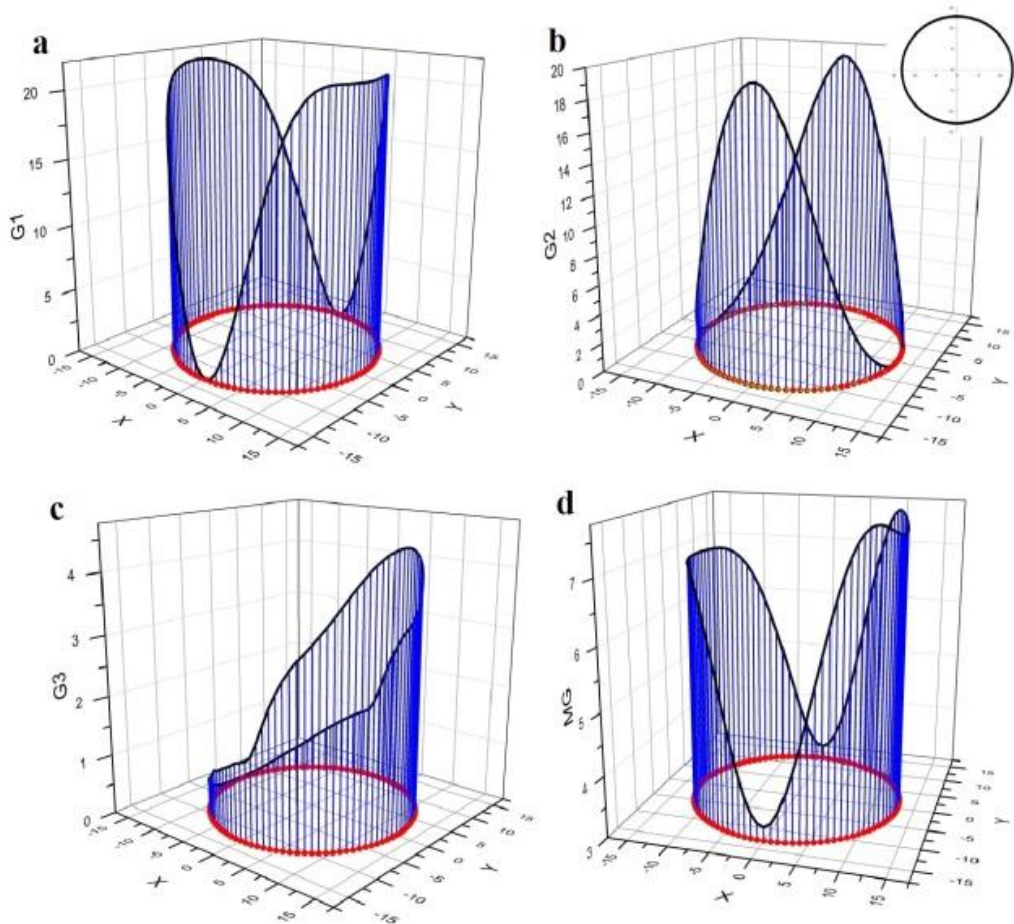

Fig. 14. Strain energy release rate curves for [90//0/0/90/90/0/0/90] stacking sequence: a- Strain energy release rate of the first mode, b- Strain energy release rate of the second mode, c- Strain energy release rate of the third mode, d- growth criteria.

The numerical results indicate that once the delamination growth stops under a displacement load of 1.9494mm, the nest load step which will lead to a progressive growth will be a displacement loading of is 1.97$mm(\dfrac{U_x}{U_{xc}} = 1.6260)$. The last load which makes the delamination growth to become unstable is 2.12$mm(\dfrac{U_x}{U_{xc}} = 1.7498)$. The process of the delamination growth for the stacking sequence of [90//0/0/90/90/0/0/90] is shown in Fig. 16. This figure indicates that the bucking mode is changed in the last steps, since the shape of the crack tip changes from symmetrical to nonsymmetrical.
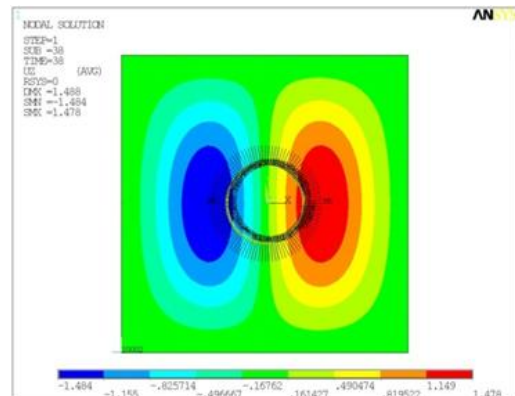

Fig. 15. Buckling mode of the plate with stacking sequence of [90//0/0/90/90/0/0/90] in the first step of delamination growth
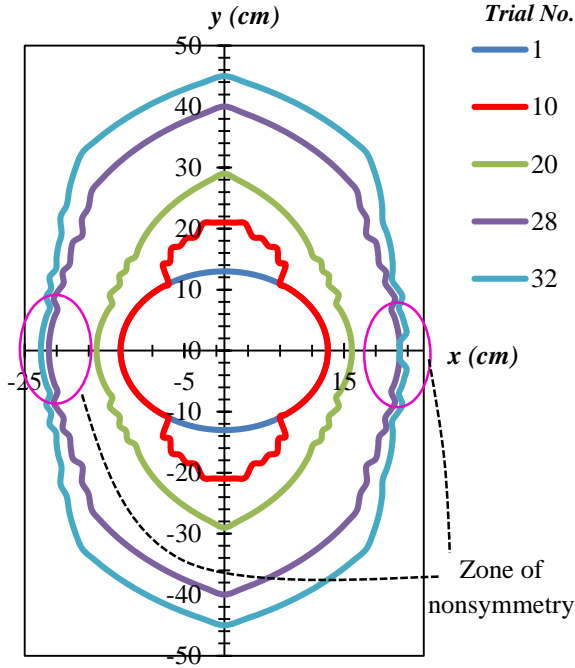
Fig. 16. Delamination growth process in [90//0/0/90/90/0/0/90] sample.

Variation in load carrying capacity versus the displacement of the right and left edges are shown in Fig. 17. Due to unstable growth of the delamination zone, the load carrying capacity experiences a sharp drop at this step of the analysis for the stacking sequence given above.
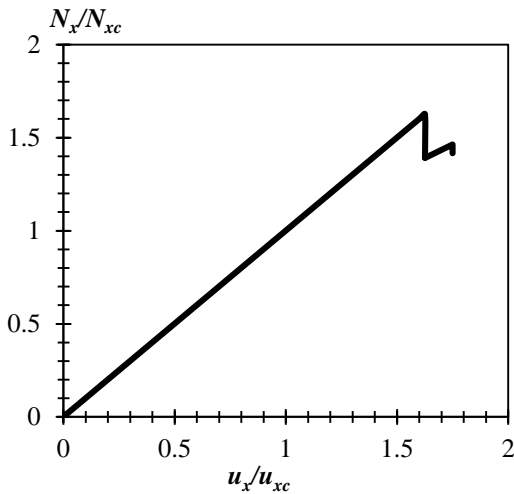

Fig. 17. Variation in force based on the edge displacement in [90//0/0/90/90/0/0/90] sample.

Fig. 18 shows that the buckling mode of the delaminated plate is changed at $\frac{U_x}{U_{xc}} = 1.65$ where delamination growth became unstable at $\frac{U_x}{U_{xc}} = 1.6$.
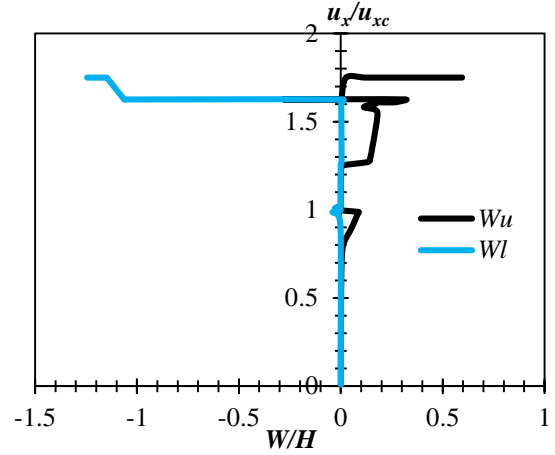

Fig. 18. Out-of-plane displacement of the node located at the center of the plate for [90//0/0/90/90/0/0/90] sample.

Comparison of the delamination growth between the three postulated samples in this work is shown in Fig. 19. The boundary of each sample ([0/90/90//0/0/90/90/0], [0//90/90/0/0/90/90/0] and [90//0/0/90/90/0/0/90]) is produced under a displacement loads of $\frac{U_x}{U_{xc}} = 0.4451$, $\frac{U_x}{U_{xc}} = 1.23$ and $\frac{U_x}{U_{xc}} = 1.75$, respectively. Delamination propagation for the stacking sequences of [0/90/90//0/0/90/90/0] and [0//90/90/0/0/90/90/0] occurs in the *x*-direction while for [90//0/0/90/90/0/0/90] layups it occurs in *y*-direction. In all three cases, the applied load acts in the *x*-direction. This figure indicates that the stacking sequence has a significant effect on the delamination growth.
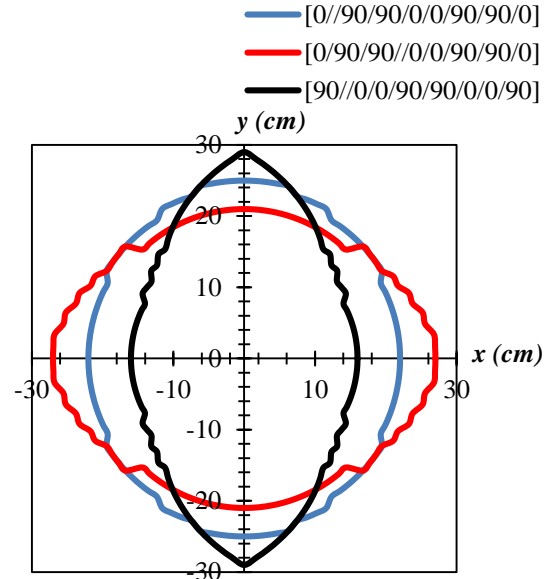

Fig. 19. Comparison of delamination growth for the three samples under different loads.

5. Conclusions

This work studied the buckling and post-buckling behavior of delaminated composite plates under compressional loading. Virtual crack closure technique was employed to investigate the delamination growth. The obtained results show that the shape of the delamination tip during its growth depends on the applied load direction at the boundaries, initial delamination shape, and it's geometrical location within the plate. Furthermore, during the delamination growth, the load carrying capacity of the plate decreases and the out-of-plane displacement of the delaminated sub-laminates changes dramatically. Additionally, according to numerical results, a delaminated composite will remain sound and stable until the crack growth become unstable. Moreover, the buckling mode of a delaminated composite plate may change with a growth in size of the delaminated zone. Additionally, any change in buckling mode often causes an unstable crack growth and a sudden drop in the load carrying capability of the overall structure. Results also show that the stacking sequence of the delaminated plate has a significant effect on the delamination growth and load carrying capacity of the composite plate.

6. References

[1] K. F. Nilsson, L. E. Asp, J. E. Alpman, L. Nystedt, Delamination buckling and growth for delaminations at different depths in a slender composite panel, *International Journal of Solids and Structures,* Vol. 38, No. 17, pp. 3039-3071, 4//, 2001.

[2] S.-F. Hwang, S.-M. Huang, Postbuckling behavior of composite laminates with two delaminations under uniaxial compression, *Composite Structures,* Vol. 68, No. 2, pp. 157-165, 4//, 2005.

[3] K. Alnefaie, Finite element modeling of composite plates with internal delamination, *Composite Structures,* Vol. 90, No. 1, pp. 21-27, 9//, 2009.

[4] I. Tawk, P. Navarro, J. F. Ferrero, J. J. Barrau, E. Abdullah, Composite delamination modelling using a multi-layered solid element, *Composites Science and Technology,* Vol. 70, No. 2, pp. 207-214, 2//, 2010.

[5] Y. Lin, Role of matrix resin in delamination onset and growth in composite laminates, *Composites Science and Technology,* Vol. 33, No. 4, pp. 257-277, 1988/01/01/, 1988.

[6] A. Turon, P. P. Camanho, J. Costa, J. Renart, Accurate simulation of delamination growth under mixed-mode loading using cohesive elements: Definition of interlaminar strengths and elastic stiffness, *Composite Structures,* Vol. 92, No. 8, pp. 1857-1864, 7//, 2010.

[7] J. D. Whitcomb, Finite element analysis of instability related delamination growth, *Journal of Composite Materials,* Vol. 15, No. 5, pp. 403-426, 1981.

[8] W. Gong, J. Chen, E. A. Patterson, Buckling and delamination growth behaviour of delaminated composite panels subject to four-point bending, *Composite Structures,* Vol. 138, pp. 122-133, 3/15/, 2016.

[9] R. G. Wang, L. Zhang, J. Zhang, W. B. Liu, X. D. He, Numerical analysis of delamination buckling and growth in slender laminated composite using cohesive element method, *Computational Materials Science,* Vol. 50, No. 1, pp. 20-31, 11//, 2010.

[10] H. Hosseini-Toudeshky, S. Hosseini, B. Mohammadi, Delamination buckling growth in laminated composites using layerwise-interface element, *Composite Structures,* Vol. 92, No. 8, pp. 1846-1856, 7//, 2010.

[11] L. G. Melin, J. Schön, Buckling behaviour and delamination growth in impacted composite specimens under fatigue load: an experimental study, *Composites Science and Technology,* Vol. 61, No. 13, pp. 1841-1852, 10//, 2001.

[12] Y. Ni, A. K. Soh, On the growth of buckle-delamination pattern in compressed anisotropic thin films, *Acta Materialia,* Vol. 69, pp. 37-46, 2014/05/01/, 2014.

[13] D. Bruno, F. Greco, An asymptotic analysis of delamination buckling and growth in layered plates, *International Journal of Solids and Structures,* Vol. 37, No. 43, pp. 6239-6276, 2000/10/25/, 2000.

[14] X. Zhang, S. Yu, The growth simulation of circular buckling-driven delamination, *International Journal of Solids and Structures,* Vol. 36, No. 12, pp. 1799-1821, 4/1/, 1999.

[15] K.-F. Nilsson, A. E. Giannakopoulos, A finite element analysis of configurational stability and finite growth of buckling driven delamination, *Journal of the Mechanics and Physics of Solids,* Vol. 43, No. 12, pp. 1983-2021, 1995/12/01/, 1995.

[16] K. F. Nilsson, J. C. Thesken, P. Sindelar, A. E. Giannakopoulos, B. Stoåkers, A theoretical and experimental investigation of buckling induced delamination growth, *Journal of the Mechanics and Physics of Solids,* Vol. 41, No. 4, pp. 749-782, 1993/04/01/, 1993.

[17] N. Chitsaz, H. R. Ovesy, M. Kharazi, Buckling and post-buckling analysis of delaminated piezo-composite material under electro-mechanical loading, *Journal of Intelligent Material Systems and Structures,* Vol. 27, No. 13, pp. 1780-1791, 2016.

[18] N. Chitsaz, H. Ovesy, M. Kharazi, Post-buckling analysis of piezo-composite laminate with through-the-width delamination based on layerwise theory, in *European conference on composite materials*, Seville, Spain, 2014.

[19] M. Kharazi, H. Ovesy, M. A. Mooneghi, Buckling analysis of delaminated composite plates using a novel layerwise theory, *Thin-Walled Structures,* Vol. 74, pp. 246-254, 2014.

[20] M. Kharazi, H. R. Ovesy, Large deflection compressional analysis of unsymmetric delaminated composite plates with consideration of contact phenomenon, *Applied Composite Materials,* Vol. 17, No. 5, pp. 515-528, 2010.

[21] M. Kharazi, H. Ovesy, Compressional Stability Behavior of Composite Plates with Multiple Through-the-Width Delaminations, *Journal of Aerospace Science and Technology,* Vol. 5, No. 1, pp. 13-22, 2008.

[22] M. Kharazi, H. Ovesy, Postbuckling behavior of composite plates with through-the-width delaminations, *Thin-Walled Structures,* Vol. 46, No. 7, pp. 939-946, 2008.

[23] T. K. O'Brien, *Characterization of delamination onset and growth in a composite laminate*, in: *Damage in Composite Materials: Basic Mechanisms, Accumulation, Tolerance, and Characterization*, Eds.: ASTM International, 1982.

[24] H. R. Asemi, S. R. Asemi, A. Farajpour, M. Mohammadi, Nanoscale mass detection based on vibrating piezoelectric ultrathin films under thermo-electro-mechanical loads, *Physica E: Low-dimensional Systems and Nanostructures,* Vol. 68, pp. 112-122, 4//, 2015.

[25] M. Mohammadi, M. Goodarzi, M. Ghayour, S. Alivand, Small scale effect on the vibration of orthotropic plates embedded in an elastic medium and under biaxial in-plane pre-load via nonlocal elasticity theory, *Journal of Solid Mechanics,* Vol. 4, No. 2, pp. 128-143, 2012.

[26] M. Mohammadi, A. Farajpour, M. Goodarzi, R. Heydarshenas, Levy type solution for nonlocal thermo-mechanical vibration of orthotropic mono-layer graphene sheet embedded in an elastic medium, *Journal of Solid Mechanics,* Vol. 5, No. 2, pp. 116-132, 2013.

[27] A. Farajpour, M. H. Yazdi, A. Rastgoo, M. Mohammadi, A higher-order nonlocal strain gradient plate model for buckling of orthotropic nanoplates in thermal environment, *Acta Mechanica,* Vol. 227, No. 7, pp. 1849-1867, 2016.

[28] M. Mohammadi, A. Farajpour, M. Goodarzi, H. Mohammadi, Temperature effect on vibration analysis of annular graphene sheet embedded on visco-pasternak foundation, *J. Solid Mech,* Vol. 5, pp. 305-323, 2013.

[29] M. Goodarzi, M. Mohammadi, A. Farajpour, M. Khooran, Investigation of the effect of pre-stressed on vibration frequency of rectangular nanoplate based on a visco pasternak foundation, *Journal of Solid Mechanics,* Vol. 6, pp. 98-121, 2014.

[30] M. Mohammadi, M. Safarabadi, A. Rastgoo, A. Farajpour, Hygro-mechanical vibration analysis of a rotating viscoelastic nanobeam embedded in a visco-Pasternak elastic medium and in a nonlinear thermal environment, *Acta Mechanica,* Vol. 227, No. 8, pp. 2207-2232, 2016.

[31] M. R. Farajpour, A. Rastgoo, A. Farajpour, M. Mohammadi, Vibration of piezoelectric nanofilm-based electromechanical sensors via higher-order non-local strain gradient theory, *Micro & Nano Letters,* Vol. 11, No. 6, pp. 302-307, 2016.

[32] S. R. Asemi, M. Mohammadi, A. Farajpour, A study on the nonlinear stability of orthotropic single-layered graphene sheet based on nonlocal elasticity theory, *Latin American Journal of Solids and Structures,* Vol. 11, No. 9, pp. 1515-1540, 2014.

[33] D. Xie, S. B. Biggers, Strain energy release rate calculation for a moving delamination front of arbitrary shape based on the virtual crack closure technique. Part I: Formulation and validation, *Engineering Fracture Mechanics,* Vol. 73, No. 6, pp. 771-785, 2006/04/01, 2006.

[34] *ANSYS web page*, Accessed; http://www.ansys.com/.